Electrical properties of bulk semi-insulating β-Ga_2O_3 (Fe)

A. Y. Polyakov, N. B. Smirnov, I. V. Shchemerov, S. J. Pearton, Fan Ren, A. V. Chernykh, and A. I. Kochkova

Citation: Appl. Phys. Lett. **113**, 142102 (2018); doi: 10.1063/1.5051986
View online: https://doi.org/10.1063/1.5051986
View Table of Contents: http://aip.scitation.org/toc/apl/113/14
Published by the American Institute of Physics

AIP | Conference Proceedings
Get 30% off all print proceedings!
Enter Promotion Code PDF30 at checkout

Electrical properties of bulk semi-insulating β-Ga_2O_3 (Fe)

A. Y. Polyakov,[1] N. B. Smirnov,[1] I. V. Shchemerov,[1] S. J. Pearton,[2,a)] Fan Ren,[3] A. V. Chernykh,[1,4] and A. I. Kochkova[1]

[1]*National University of Science and Technology MISiS, 4 Leninskiy Ave., Moscow 119049, Russia*
[2]*Department of Materials Science and Engineering, University of Florida, Gainesville, Florida 32611, USA*
[3]*Department of Chemical Engineering, University of Florida, Gainesville, Florida 32611, USA*
[4]*Pulsar Scientific and Production Enterprise, Joint Stock Company, Okruzhnoy Way, House 27, Moscow 105187, Russia*

(Received 13 August 2018; accepted 21 September 2018; published online 4 October 2018)

The Fermi level in bulk semi-insulating β-Ga_2O_3 doped with Fe ($\sim 5 \times 10^{18}$ cm^{-3}) is found to be pinned near $E_c - 0.85$ eV. At temperatures $\geq$400 K, Ni Schottky diodes showed good rectification and measurable low frequency capacitance, allowing the measurement of capacitance-frequency (C-f), capacitance-voltage (C-V), and capacitance-temperature (C-T) characteristics. The activation energy and the electron capture cross section obtained were (0.75–0.82) eV and (2–5) $\times 10^{-15}$ cm^2, in good agreement with the reported signature of the E2 electron trap assigned to Fe. The concentration of the filled centers determined from C-V was close to the concentration of residual shallow donors in undoped materials. Photoinduced current transient spectroscopy measurements showed that Fe doping does not promote the generation of high densities of deep traps other than those related to Fe. *Published by AIP Publishing.* https://doi.org/10.1063/1.5051986

β-Ga_2O_3 is rapidly emerging as a next generation wide-bandgap material with very promising properties for use in high-power/high-temperature transparent field effect transistors (FETs) and rectifiers.[1–3] The large direct bandgap of 4.8 eV, high electric breakdown field of 8 MV/cm, and high electron saturation velocity of $\sim 2 \times 10^7$ cm/s combined with the availability of the high crystalline quality (dislocation density $< 10^4$ cm^{-2}) bulk and epitaxial n-type material have led to demonstrations of power rectifiers,[2,3] metal-semiconductor field effect transistors (MESFETs),[4–6] FETs with insulated gate (MISFETs),[7,8] nanobelt back-gated MISFETs,[9,10] and heterojunction nanobelt JFETs[11] with excellent characteristics. A key building block in lateral FET applications is a high resistivity buffer. Since undoped crystals and films of β-Ga_2O_3 are commonly n-type, with electrons provided by Sn, Si, or Ge doping,[2] deep compensating acceptors at concentrations higher than those of the residual donors are required in order to pin the Fermi level far away from the conduction band edge in semi-insulating buffers. Currently, two acceptor impurities, Fe and Mg, have been successfully employed to compensate the residual n-type conductivity in bulk crystals and epitaxial films of β-Ga_2O_3 used as semi-insulating buffers in FETs.[12–16] Theory predicts Mg to occupy two Ga sites and to form deep acceptor states near $E_v + 1.27$ eV and $E_v + 1.06$ eV, respectively.[15] Strong complexing of the Mg with hydrogen donors and with Ir contamination from crucibles has been reported.[15]

Fe ions in β-Ga_2O_3 are known to occupy the two non-equivalent Ga(I) and Ga(II) sites, with Fe in the Ga(II) site being the dominant species.[16–18] The respective levels in the bandgap are expected to be close to each other and located in the vicinity of $E_c - 0.6$ eV.[16] High temperature Hall measurements on Ga_2O_3 (Fe) showed an acceptor level at $E_C - 0.86$ eV,[19] with the material remaining weakly n-type at 400 K and not all the Fe being electrically active. Deep level transient spectroscopy (DLTS) of bulk Czochralski grown β-Ga_2O_3 crystals revealed dominant electron traps with levels near $E_c - (0.74–0.82)$ eV, so-called E2 traps believed to be major compensating centers in the bulk material.[18–20] For Halide Vapor Phase Epitaxy (HVPE) films, a good correlation was observed between the density of the E2 traps and the concentration of Fe, while the E2 concentration did not change upon proton irradiation.[21] This suggested that the E2 traps could correspond to the charge transfer level Fe^{2+}/Fe^{3+} in β-Ga_2O_3.[20] In contrast, the density of other traps with levels close to E2, so called E2* traps, rapidly increased with proton irradiation,[19,20] indicating that native defects participate in their formation. Once the concentration of Fe doping in edge-defined film-fed grown (EFG) bulk crystals exceeded the concentration of residual donors ($\sim 2 \times 10^{17}$ cm^{-3}), the material becomes semi-insulating (SI), with a room temperature resistivity of $\sim 10^{12}$ Ωcm.[22] Fe doped EFG SI substrates are commercially available[22] and have been used as buffers to fabricate β-Ga_2O_3 FETs.[7] However, electron trapping in the buffers of such FETs is a concern and gives rise to prominent current collapse.[7] Analysis of the transient behavior of FETs indicates the participation of traps similar to the E2 traps and suggests that more work is needed on the position of Fermi level pinning in the material, the concentration of traps pinning the Fermi level and filled with electrons, and finally, the spectra of other deep traps present in the SI material. In this letter, we report these properties in EFG SI-Ga_2O_3 doped with Fe.

The (010) crystals were acquired from Tamura Corp. (Japan) and grown by EFG and doped with Fe to a concentration exceeding the background donor doping of $\sim 2 \times 10^{17}$ cm^{-3}. For contact preparation, the samples were degreased in organic solvents and the surfaces treated in Ar plasma (40 mTorr, 150 W, self-bias 320 V) for 1.5–2 min. Ohmic contacts to front and back surfaces on one type of sandwich structure were made by e-beam deposition of Ti/Au (20 nm/

a)Author to whom correspondence should be addressed: spear@mse.ufl.edu

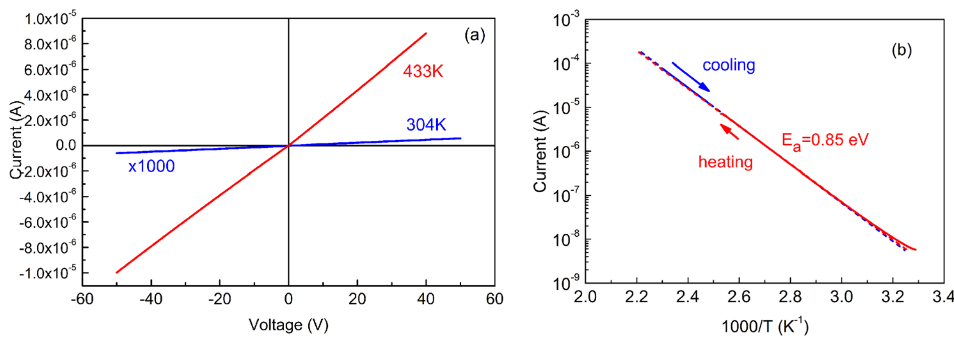

FIG. 1. (a) Current voltage characteristics for Ohmic contacts (sandwich configuration) for temperatures of 433 K and 304 K (the latter is multiplied by 1000 to bring the data into scale with the high-temperature line): (b) temperature dependence of current at −50 V measured during heating up (red curve) and cooling down (blue curve).

50 nm) in a vacuum of 2×10^{-7} Torr annealed at 470 °C for 1.5 min in N_2. Using this technique, two Ohmic contacts strips with dimensions of $7 \times 2\,mm^2$ and the whole area back contact were formed. Schottky diodes on another type of structure were prepared by Ni deposition through a shadow mask (Ni thickness: 20 nm; diameter of the diodes: 1.25 mm), with the annealed Ti/Au as a back Ohmic contact.

The current voltage (I-V) and temperature dependence of current (I-T) in the sandwich arrangement of the Ohmic contacts (i.e., between one of the top Ohmic contacts and the bottom contact) were measured from 77–400 K (Oxford Instruments gas-flow cryostat) or 290–470 K (hot stage). For the Schottky diodes, we measured I-V characteristics in the dark and under illumination with high-power (optical power 250 mW) light emitting diodes (LEDs) (wavelength from 940 nm to 365 nm), capacitance versus frequency (C-f) characteristics in the dark and under illumination, C-V characteristics, capacitance-temperature at different frequencies (admittance spectra), and photoinduced current transient spectra (PICTS).[23] For these experiments, an automated setup based on B2902A current/voltage source/meter, E4980A LCR meter (Keysight Technology, USA), was used.[24,25] The current could be measured with a resolution of 100 fA at voltages up to 100 V; in current relaxation measurements in PICTS, the entire photocurrent relaxation curve was monitored and stored at each temperature point, the temperature ramp was typically 1 K/min, the temperature step was typically 0.1 K, the temperature was controlled and regulated with an accuracy of 0.1 K, and the lowest time step during the relaxation curves measurements was 0.1 ms. The capacitance was measured in the frequency range of 20 Hz–1 MHz. Due the high series resistance of the diodes, the series equivalent circuit was used and C-V measurements were performed at frequencies where the capacitance approached a plateau and the quality factor was >2.

The I-V characteristics of the Ohmic contacts were quite linear for ≥300 K. The resistivity was estimated from measurements between one of the top contacts and the bottom contact, and it was similar for both contacts and was 2.5×10^{11} Ω cm at 300 K and 1.6×10^{7} Ω cm at 430 K, assuming that the sample is electrically uniform and taking into account the contact geometry. The room temperature value corresponds to an Fe concentration of $\sim 5 \times 10^{17} cm^{-3}$.[23] The temperature dependence of current was exponential, with an activation energy of 0.85 eV, showing no hysteresis for measurements with heating up and cooling down [see Figs. 1(a) and 1(b)]. This suggests that the Fermi level in Ga_2O_3 (Fe) semi-insulator is pinned near $E_c - 0.8$ eV, i.e., close to the E2 trap associated with Fe.[20]

For the Schottky diodes, the I-V characteristics at 300 K showed no rectification because the current was determined by the series resistance of the quasi-neutral region. At high temperatures, the rectification was as expected for a Schottky diode on a high-resistivity n-type material. Illumination with intense light produced measurable photocurrent and the I-V curve showed a positive open-circuit voltage [the 460 K I-V curve measured in the dark and under illumination with high-power LED with a peak photon energy of 3.4 eV is shown in Fig. 2(a)]. Measurements of the spectral dependence of photocurrent normalized to dark current showed an optical threshold near 1.5 eV and a strong photocurrent band with the optical threshold between 2 eV and 2.3 eV [Fig. 2(b)]. The lower threshold is likely due to electron excitation over the Schottky barrier. The 2.3 eV optical threshold is close to the one observed in deep level optical spectroscopy (DLOS)[19] and in photocapacitance/light C-V spectra of lightly doped n-type samples[19,21,25] and was attributed to unidentified deep acceptor states near $E_c - 2$ eV.[19] These Schottky diodes displayed a measurable capacitance at low frequencies, and the C-f characteristics showed a plateau for frequencies up to 100 Hz at 460 K [Fig. 3(a)]. As the temperature decreased, the capacitance first did not change and then decreased, showing a step [see the inset in Fig. 3(a)]. The temperature corresponding

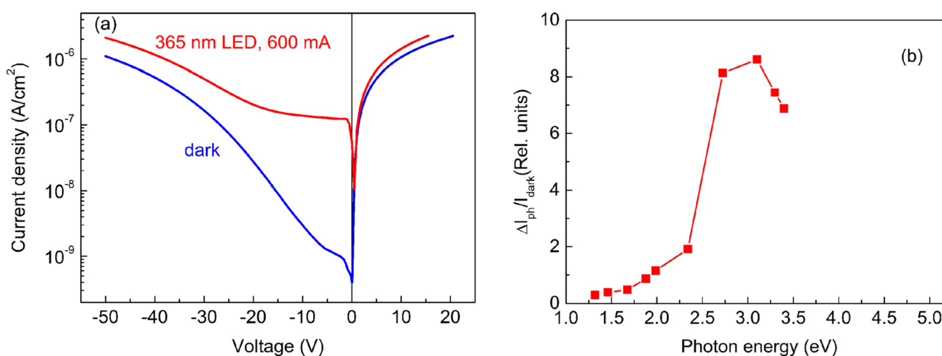

FIG. 2. (a) 460 K current voltage characteristic of the Schottky diode measured in the dark (blue curve) and under illumination with 365 nm (3.4 eV) LED (red curve); (b) photocurrent normalized to the dark current spectrum at −10 V.

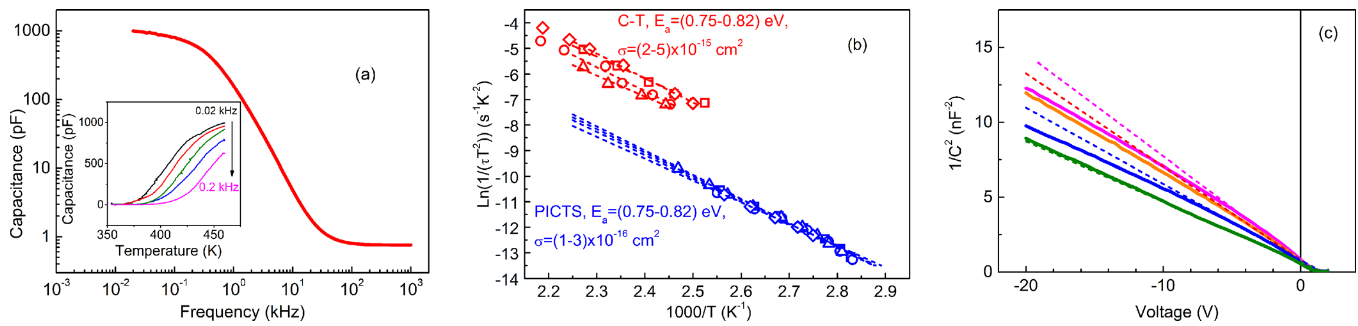

FIG. 3. (a) C-f characteristics of one of the studied Schottky diodes measured at 460 K; the inset shows the temperature dependence of capacitance at several measurement frequencies from 0.02 kHz to 0.2 kHz; (b) Arrhenius plots of the main center observed in C-T and PICTS measurements with 365 nm LED excitation (the data show the spread for the four diodes measured); (c) dark (orange and olive lines) $1/C^2$ plots of two Schottky diodes; magenta and blue lines correspond to the plots obtained under 365 nm LED excitation; the dashed curves present the slope of the $1/C^2$ versus voltage dependence near the surface.

to the middle of the step became lower as the measurement frequency decreased, as expected in admittance spectroscopy.[26] This shift of the temperature position of the step with frequency allows the determination of the position of the energy level pinning the Fermi level from the Arrhenius plot of $1/(\tau T^2)$ versus 1000/T (T is the temperature of the step and $\tau = 1/2\pi f$, with f being the probing frequency in capacitance measurements). Figure 3(b) displays the Arrhenius plots obtained for four separate Schottky diodes. The activation energy and the electron capture cross section obtained were (0.75–0.82) eV and $(2\text{–}5) \times 10^{-15}$ cm^2. These are in good agreement with the reported signature of the E2 electron trap assigned to Fe.[19] The space charge in capacitance measurements on these high-resistivity Schottky diodes is due to the difference in occupation of the E2 traps in the quasi-neutral region (these deep acceptors are partly filled with electrons coming from the shallow donors) and in the space charge region where the E2 traps are empty. The step in capacitance appears as a result of electrons on the traps not being able to follow the probing frequency.[26] Then, in C-V characteristics measured at low frequencies on the plateau in C-f dependence, the slope of $1/C^2 - V$ yields the concentration of electrons residing on the E2 traps. Such $1/C^2$ (V) plots are shown for two diodes in Fig. 3(c). The plots are not quite linear and show a lower concentration in the near-surface region compared to deeper part of the sample (1.3×10^{17} cm^{-3} versus 1.8×10^{17} cm^{-3} for one diode and 1.7×10^{17} cm^{-3} versus 2.3×10^{17} cm^{-3} for the other). The concentrations in both regions differ by about 1.3 times for the two Schottky diodes, indicating local differences in the residual donor concentrations in the sample.

Illumination produced an increase in photocapacitance and in the C-V concentration due to the ionization of deeper traps. The changes in photocapacitance started for photon energies >2 eV. Figure 3(c) displays the $1/C^2 - V$ characteristics of Schottky diodes under illumination with an LED with a photon energy of 3.4 eV. The concentration increased by $2\text{–}4 \times 10^{16}$ cm^{-3} within four Schottky diodes measured. This is due to the ionization of the acceptors with optical excitation threshold near 2.3 eV, similar to the $E_c - 2$ eV acceptors in DLOS.[18] The acceptor concentrations are about an order of magnitude higher than the concentrations of the $E_c - 2$ eV traps deduced for bulk n-Ga_2O_3 samples by DLOS/photocapacitance.[19]

We also examined whether E2 traps were the only prominent deep centers present because heavy Fe doping can promote the formation of other defects. This was done by measurements of PICTS spectra.[23,24] With 3.4 eV excitation, measurements were done at a reverse bias of −10 V and the peaks in the spectra obtained by plotting the difference in the transient current values at time windows t_1 and t_2 ($t_2 \gg t_1$) after the end of the pulse. With $\Delta I = I(t_1) - I(t_2)$, the signal was normalized to the steady-state photocurrent I_{ph} during the pulse to account for the product of mobility and lifetime variation with temperature.[23,24] Measurable photocurrent was only obtained for temperatures >300 K. The spectra displayed a single well defined peak (Fig. 4) allowing determination of the energy level position and the carrier capture cross section from the Arrhenius plot of $1/(\tau T^2)$ versus 1000/T (T is the temperature of the peak for time windows set of t_1 and t_2, $\tau = 1/t_1$[23,24]). This Arrhenius plot is shown in Fig. 3(b) together with the plots derived from C-T measurements. The activation energies were in the range $E_a = (0.75\text{–}0.82)$ eV, with cross sections of $(1\text{–}3) \times 10^{-16}$ cm^2. The activation energies are close to those determined from C-T measurements, while the capture cross sections are lower, possibly a consequence of the difference in measurement techniques.[23,24] Capture cross sections determined from C-T should be closer to the trap parameters calculated from DLTS spectra. Both in C-T and in PICTS, we observe the same dominant center that pins the Fermi level in the SI β-Ga_2O_3 and is responsible for the activation energy of 0.85 eV

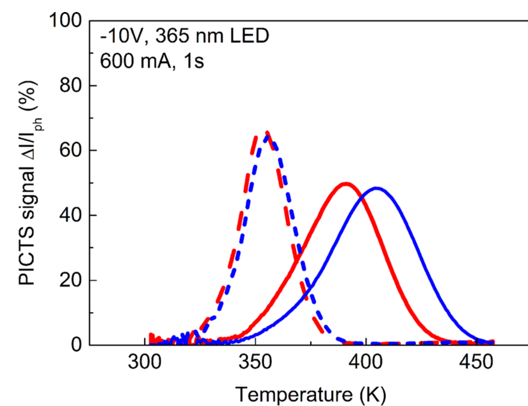

FIG. 4. PICTS spectra from a Schottky diode with 365 nm LED excitation, the PICTS signal ΔI is normalized to photocurrent Iph, pulse length of 1 s, and spectra are shown for t_1/t_2 equal to 40 ms/200 ms (blue solid line), 100 ms/500 ms (red solid line), 1360 ms/6800 ms (blue dashed line), and 1700 ms/8500 ms (red dashed line).

in Ohmic conductivity. The parameters of the center deduced from C-T measurements are close to those of the E2 electron trap attributed to Fe.[20] In undoped or lightly doped n-Ga_2O_3 bulk crystals, the E2 centers are commonly dominant, with a concentration of $\sim 10^{16}$ cm^{-3}.

Two other often observed centers E1 ($E_c - 0.6$ eV) and E3 ($E_c - 1$ eV) usually have lower concentrations of mid-10^{14} cm^{-3} (E1) or mid-10^{15} cm^{-3} (E3),[18,19] although in some bulk or HVPE samples, the E3 concentration is comparable to E2.[18,21] These traps are known to be related to native point defects produced by irradiation.[21] In the PICTS spectra, we do not see indications of the presence of these additional traps in quantities comparable to the density of the dominant trap, which suggests that the incorporation of a high concentration of Fe does not provoke the formation of lattice defects giving rise to the E1 and E3 centers.

Hole traps in undoped or lightly doped n-Ga_2O_3 are mainly of two kinds, with an optical threshold of 2.1–2.3 eV (our E_c -2 eV traps) observed in DLOS/photocapacitance/light C-V spectra with a concentration of $\sim 10^{15}$ cm^{-3} and hole traps near E_v + (1.3–1.4) eV (H3 traps[27]) observable by optical DLTS and light C-V measurements.[27] The latter traps were not seen in our PICTS spectra, suggesting that their concentration is low compared to that of the main center introduced by Fe doping. While the hole emission from the E_c -2 eV hole traps cannot be detected by PICTS in our temperature region, these most likely are the traps giving rise to the photocapacitance and photocurrent of the Schottky diodes at high temperatures. Their concentration is higher than in undoped bulk crystals, $\sim 10^{16}$ cm^{-3}, which could be related to defect formation upon Fe doping.[28]

In conclusion, heavy Fe doping used to obtain semi-insulating bulk β-Ga_2O_3 does not induce the formation of high densities of deep electron and hole traps other than the center near $E_c - 0.8$ eV ascribed to Fe. With the high Fe concentrations used to compensate shallow donors in bulk undoped EFG crystals, the density of the empty Fe states available for trapping in FETs on these buffers will always produce current collapse in the pulsed operation mode. The situation might be improved by using HVPE buffers with a lower residual donor concentration grown on bulk SI-Ga_2O_3 (Fe) substrates.[21] If doped with Fe to achieve high resistivity, such buffers would require much lower Fe concentration and mitigate trapping.

The work at NUST MISiS was supported in part by the Ministry of Education and Science of the Russian Federation in the framework of Increase Competitiveness Program of NUST (MISiS) (K2-2014-055). The work at UF was sponsored by the Department of Defense, Defense Threat Reduction Agency, HDTRA1-17-1-011, monitored by Jacob Calkins.

[1] M. A. Mastro, A. Kuramata, J. Calkins, J. Kim, F. Ren, and S. J. Pearton, ECS J. Solid State Sci. Technol. **6**, P356 (2017).
[2] M. Higashiwaki and G. H. Jessen, Appl. Phys. Lett. **112**, 060401 (2018).
[3] S. J. Pearton, J. Yang, P. H. Cary, F. Ren, J. Kim, M. J. Tadjer, and M. A. Mastro, Appl. Phys. Rev. **5**, 011301 (2018).
[4] K. Sasaki, M. Higashiwaki, A. Kuramata, T. Masui, and S. Yamakoshi, J. Cryst. Growth **378**, 591 (2013).
[5] M. Higashiwaki, K. Sasaki, T. Kamimura, M. H. Wong, D. Krishnamurthy, A. Kuramata, T. Masui, and S. Yamakoshi, Appl. Phys. Lett **103**, 123511 (2013).
[6] H. Zhou, M. Si, S. Alghamdi, G. Qiu, L. Yang, and P. D. Ye, IEEE Electron Device Lett. **38**, 103 (2017).
[7] J. F. McGlone, Z. Xia, Y. Zhang, C. Joishi, S. Lodha, S. Rajan, S. A. Ringel, and A. R. Arehart, IEEE Electron. Devices Lett. **39**, 1042 (2018).
[8] M. J. Tadjer, N. A. Mahadik, V. D. Wheeler, E. R. Glaser, L. Ruppalt, A. D. Koehler, K. D. Hobart, C. R. Eddy, and F. J. Kub, ECS J. Solid State Sci. Technol. **5**, P468 (2016).
[9] J. Kim, S. Oh, M. A. Mastro, and J. Kim, Phys. Chem. Chem. Phys. **18**, 15760 (2016).
[10] J. Kim, M. A. Mastro, M. J. Tadjer, and J. Kim, ACS Appl. Mater. Interfaces **9**, 21322 (2017).
[11] J. Kim, M. A. Mastro, M. J. Tadjer, and J. Kim, ACS Appl. Mater. Interfaces **10**, 29724 (2018).
[12] Z. Galazka, K. Irmscher, R. Uecker, R. Bertram, M. Pietsch, A. Kwasniewski, M. Naumann, T. Schulz, R. Schewski, D. Klimm, and M. Bickermann, J. Cryst. Growth **404**, 184 (2014).
[13] T. Onuma, S. Fujioka, T. Yamaguchi, M. Higashiwaki, K. Sasaki, T. Masui, and T. Honda, Appl. Phys. Lett. **103**, 041910 (2013).
[14] B. E. Kananen, L. E. Halliburton, E. M. Scherrer, K. T. Stevens, G. K. Foundos, K. B. Chang, and N. C. Giles, Appl. Phys. Lett. **111**, 072102 (2017).
[15] J. R. Ritter, J. Huso, P. T. Dickens, J. B. Varley, K. G. Lynn, and M. D. McCluskey, Appl. Phys. Lett. **113**, 052101 (2018).
[16] M. L. Meilman, Sov. Phys. Solid State **11**, 1403 (1969) [Fiz. Tverd. Tela **11**, 1730 (1969)].
[17] R. Büscher and G. Lehmann, Z. Naturforsch. **42a**, 67 (1987).
[18] K. Irmscher, Z. Galazka, M. Pietsch, R. Uecker, and R. Fornari, J. Appl. Phys. **110**, 063720 (2011).
[19] A. T. Neal, S. Mou, S. Rafique, H. Zhao, E. Ahmadi, J. S. Speck, K. T. Stevens, J. D. Blevins, D. B. Thomson, N. Moser, K. D. Chabak, and G. H. Jessen, Appl. Phys. Lett. **113**, 062101 (2018).
[20] Z. Zhang, E. Farzana, A. R. Arehart, and S. A. Ringel, Appl. Phys. Lett. **108**, 052105 (2016).
[21] M. E. Ingebrigtsen, J. B. Varley, A. Y. Kuznetsov, B. G. Svensson, G. Alfieri, A. Mihaila, U. Badstübner, and L. Vines, Appl. Phys. Lett. **112**, 042104 (2018).
[22] A. Y. Polyakov, N. B. Smirnov, I. V. Shchemerov, E. B. Yakimov, J. Yang, F. Ren, G. Yang, J. Kim, A. Kuramata, and S. J. Pearton, Appl. Phys. Lett. **112**, 032107 (2018).
[23] A. Kuramata, K. Koshi, S. Watanabe, Y. Yamaoka, T. Masui, and S. Yamakoshi, Proc. SPIE **10533**, 105330E (2018).
[24] M. Tapiero, N. Benjelloun, J. P. Zielinger, S. El Hamd, and C. Noguet, J. Appl. Phys. **64**, 4006 (1988).
[25] A. Y. Polyakov, N. B. Smirnov, I. V. Shchemerov, D. Gogova, S. A. Tarelkin, I.-H. Lee, and S. J. Pearton, ECS J. Solid State Sci. Technol. **7**, P260 (2018).
[26] A. Y. Polyakov, N. B. Smirnov, I. V. Shchemerov, D. Gogova, S. A. Tarelkin, and S. J. Pearton, J. Appl. Phys. **123**, 115702 (2018).
[27] L. Pautrat, B. Katircioglu, N. Magnea, D. Bensahel, J. C. Pfister, and L. Revoil, Solid-State Electron. **23**, 1159 (1980).
[28] A. Y. Polyakov, N. B. Smirnov, I. V. Shchemerov, S. J. Pearton, F. Ren, A. V. Chernykh, P. B. Lagov, and T. V. Kulevoy, APL Mater. **6**, 096102 (2018).